Supplementary section: Ubiquitin Binding Domains

Ubiquitin recognition at the plasma membrane

The Ub-binding endocytic adaptor proteins Epsin and Eps15 are first point of contact between a freshly ubiquitinated plasma membrane receptor such as EGFR. (**Figure S1*a***). Human Epsin contains two or three UIMs (depending on the splice variant) immediately C-terminal to its Epsin N-terminal homology (ENTH) domain. Yeast has two Epsin homology, Ent1 and Ent2, both of which also have two UIMs. Human Eps15 has two UIMs at its C-terminus, while its yeast counterpart, Ede1, has a C-terminal ubiquitin associated (UBA) domain instead. UBA domains are a large family of three-helix bundles that bind ubiquitin, ubiquitin-like proteins (UBLs), other proteins, and each other with a wide range of affinities.

UIMs are among the simplest of all the UBDs, consisting of a single α-helix. The UIM consensus sequence is *X*-**Ac**-**Ac**-**Ac**-**Ac**-Φ-*X*-*X*-**Ala**-*X*-*X*-*X*-**Ser**-*X*-*X*-**Ac**-*X*-*X*-*X*-*X,* where X is any residue, Φ is a large hydrophobic residue, usually a Leu, and Ac is a acidic residue (Asp or Glu) (13). The affinities of UIMs for ubiquitin in solution are low, not exceeding 200 μM (10). The Eps15 UIMs are even weaker ubiquitin binders than most. Eps15 UIM1 (first UIM) binds ubiquitin with 0.9 mM affinity, and Eps15 UIM2 (second UIM) has nearly undetectable binding (10). No structures are available for the Eps15 or Epsin UIMs, but the first UIM of the yeast ESCRT-0 subunit Vps27 and that of the proteasome subunit S5a have both been solved by NMR in complex with ubiquitin (**Figure S1*b***) (47, 49). The conserved acidic residues interact with a basic patch made up of Arg42 and Arg72. The conserved Ala and hydrophobic residue of the UIM bind to the key Ile44 hydrophobic patch on Ub. The conserved Ser hydrogen bonds with the main

chain in the Ala46-Gly47 region (47). These principles likely apply broadly to other UIMs, with some interesting elaborations- the inverted and the double-sided UIMs- described below.

The UBA domain of the yeast Eps15 ortholog Ede1 has been analyzed structurally with ubiquitin (**Figure S1*c***) (46). The Ede1 UBA binds to the ubiquitin Ile44 patch primarily via the UBA hydrophobic motif MGF between helices α1 and α2. The ubiquitin affinity is low in comparison to some other UBA domains at ~80 μM, though this is still tighter than the binding to UIMs. The Ede1 UBA domain has a polar Thr residue in the ubiquitin binding interface that actually serves to lower its affinity for Ub. Thus the UIM and UBA domains involved in the most upstream interactions with ubiquitinated plasma membrane proteins appear to have evolved to bind ubiquitin with exceptionally low affinity, even by the standards of UBDs.

Ubiquitin recognition at post-Golgi vesicles and early endosomes

Ubiquitinated cargoes are recognized by human GGA3 (32), yeast Gga1 and Gga2 (5, 8, 38), and the Gga-like Tom1/Tom1L1-family proteins (17, 31). Human GGA3 in particular is important for the efficient passage of EGFR through the early endosome (32). These proteins all have in common Ub-binding VHS (36) and GAT (23, 38, 40) domains. VHS domains are eight-helix bundles (22, 24), and almost all of them bind ubiquitin via their α2 and α4 helices (14, 36) (**Figure S1*d***), with the exception of the VHS domains of human GGA1 and GGA2 that do not bind ubiquitin (36).

GAT domains are elongated three-helix bundles (6, 29, 39, 51) that bind two ubiquitin moieties at two different sites (5) (**Figure S1*e***), both with relatively low 200-

400 μM affinity (1, 18, 28). In the case of GGA3 site 1, which is composed of residues from helices α1 and α2, binds with ~3-fold higher affinity than site 2. Site 2 is on the opposite face of the GAT domain and consists of residues from α2 and α3(18). Tom1-GAT has the opposite pattern, with site 2 binding more tightly than site 1 (1). Nevertheless, in all available crystal structures of GAT-ubiquitin complexes, only the site 1 interaction is visualized in the crystal (1, 18, 28).

Ubiquitinated cargo is clustered on early endosomes by ESCRT-0 for entry into the MVB pathway (4, 33, 42) .ESCRT-0 consists of one copy each (30, 35) of two subunits, Hrs and STAM, known as Vps27 and Hse1 in yeast. Much like the GGAs and Tom1 family proteins, the subunits of ESCRT-0 contain multiple UBDs in their N-terminal regions. Both subunits have N-terminal VHS domains that bind ubiquitin (14, 25, 36) and both subunits also contain functional UIMs (4, 10, 33, 42, 47). The structures and affinities of the ESCRT-0 VHS and UIM domains are much as described above, with the most interesting exception being the presence of a single double-sided UIM (DUIM) in Hrs (11). In the remarkable Hrs DUIM structure, the solvent-exposed "X" residues of the motif encode a second UIM consensus sequence interwoven with the first. The single DUIM helix is thus sandwiched between two ubiquitin moieties (**Figure S1*f***).

The presence of five UBDs within an ESCRT-0 complex contributes to avid binding to polyubiquitin chains, although only to a modest degree (36). ESCRT-0 and various multiple UBD fragments of it bind Lys63-Ub_2 with 4 to 9-fold higher affinity than to monoUb, and with ~3 to 4-fold higher affinity than to Lys63-Ub_2 (36). At the tetraubiquitin level, the affinity gain for Lys63-Ub_4 over monoubiquitin increases to as much as 50-fold, but the preference for Lys63- vs. Lys48-Ub_4 decreases to at most ~ 2-

fold. ESCRT-0 binds to Lys63-Ub_4 with K_d = 18 μM, which is still substantially higher than the cellular concentration of cargoes such as EGFR, ENaC, and Cps1. More insight into how low abundance cargoes can be recognized in cells by low affinity UBD proteins comes from analysis of membrane-tethered cargoes in vitro. ESCRT-0 binds tightly to PI(3)P-containing membranes via its FYVE domain (34). When a model ubiquitin cargo is tethered to synthetic membranes at a bulk concentration of 65 nM, the cargo binds to and is clustered by 15 nM ESCRT-0 (50). Thus membrane tethering seems to be the major factor in explaining how membrane trafficking proteins that contain low-affinity UBDs are still able to interact with scarce ubiquitinated membrane proteins. Avid binding to polyubiquitinated cargo seems likely to be of secondary importance by comparison.

Mechanisms of RAB5 pathway regulation by ubiquitin

The presence of the GTP-bound form of RAB5 (Vps21 in yeast) is a defining characteristic of early endosomes. Ubiquitinated cargo is connected to the GTP occupancy of RAB5 because ubiquitin binds to its exchange factor Rabex-5 (Vps9 in yeast). The conserved RAB5 GEF domain of these proteins is known as a "VPS9 domain" (**Figure S2*a***). Despite their common function, yeast and human Rabex-5 orthologs bind ubiquitin in different ways. Yeast Vps9 binds to ubiquitin through a C-terminal CUE domain (7, 9, 43). The Vps9 CUE domain forms a domain-swapped dimer that wraps around Ub, contacting two of the three major hydrophobic patches, those surrounding Ile36 and Ile44 (**Figure S2*b***) (29). The dimerization and multiple points of contact with ubiquitin lead to a high-affinity interaction with Kd ~ 1 μM (29). The CUE domain monomer consists of a three-helix bundle similar to the UBA domain (16, 29).

Most CUE domains, excepting that of Vps9, are monomers and bind to the Ile44 patch only, using a mode of interaction similar to that of UBA domains (16).

Human Rabex-5 lacks a CUE domain, but contains two tandem UBDs at its N-terminus, a zinc finger similar to those of A20 (A20 ZnF) and an inverted UIM (MIU) (21, 26). The A20 domain binds with ~ 20 μM affinity to a predominantly polar patch surrounding Asp58 of Ub, and is the only known example of a UBD involved in membrane traffic that does not bind to the Ile44 patch (**Figure S2*c***) (21, 26). The MIU binds with ~ 30 μM affinity to the Ile44 patch. The sequence is essentially an inversion of the UIM sequence, and it binds to ubiquitin in essentially the same region of space, but with the opposite N-to-C orientation as the UIM (**Figure S2*d***). Both motifs are centered on an Ala that contacts ubiquitin Ile44. Both have acidic subdomains, but in the MIU, the acidic residues are in the C-terminal third of the helix instead of the N-terminal region. The UIM and MIU pair make a remarkable example of convergent evolution. The ubiquitin interactions with Rabex-5 and Vps9 are important for trafficking cargoes such as EGFR (26) and Ste3 (29), but it is unknown whether regulation occurs by modulating the VPS9 domain's catalytic activity or substrate binding, by recruitment to endosomes, or by other mechanisms.

Ubiquitin and multivesicular bodies

ESCRT-I and –II assemble together on endosomal membranes, bind ubiquitinated cargo, and drive intralumenal budding of the membrane. The major ubiquitin recognition site on ESCRT-I is the ubiquitin E2 variant (UEV) domain of the TSG101 subunit (Vps23 in yeast) (**Figure S3*a***). UEV domains are enzymatically inactive counterparts of ubiquitin

E2 enzymes. The TSG101 UEV domain binds to the Ile44 patch with a typical low affinity of ~0.5 mM (27) (**Figure S3*b***). Despite the similarity of the UEV fold to ubiquitin E2 enzymes, the ubiquitin binding mode is completely distinct from that of E2 enzymes (45, 48). In addition to the Ile44 patch, ubiquitin also interacts with the UEV domain via the polar region near Lys63, although Lys63 itself is not involved in direct contacts (45, 48). The binding site for the P(S/T)XP motif of ESCRT-0 and other ESCRT-I interactors does not overlap with that of Ub, allowing simultaneous binding of ubiquitin and ESCRT-0. The flexible residues at the C-terminus of the yeast ESCRT-I subunit Mvb12 also contribute to ubiquitin binding (41), though the structure of this complex is not known. The Mvb12 C-terminus is close to the UEV domain in the three-dimensional structure of ESCRT-I (19), suggesting that these regions could potentially cooperate in binding to a single polyubiquitin chain (15), or to a multiubiquitinated form of a single cargo molecule.

Yeast and human ESCRT-II both bind Ub, but they do so in different ways. The Vps36 subunit of yeast ESCRT-II contains two Npl4 zinc finger (NZF) domain, and the second NZF binds ubiquitin (3). The structure of the ESCRT-II NZF2 has not been determined in complex with Ub, but the related structure of the Npl4 NZF provided a model, showing that like other ESCRT UBD interactions, the Ile44 patch of ubiquitin was directly involved (3). More recently, the Vps36 NZF2 was shown to be part of a subgroup of NZF domains that have two ubiquitin binding surfaces. The Vps36 NZF2 domain uses these surfaces to bind to Lys63-ubiquitin chains with very high selectivity and an affinity of 380 nM by one report (20), while another study found non-selective binding to a variety of ubiquitin chains (37). The structure of the NZF domain of another

member of this subgroup, TAB2, provides a model for the ESCRT-II NZF2-Lys63-ubiquitin complex (20, 37) (**Figure S3*c***). The human ortholog of Vps63 is EAP45, which binds to ubiquitin through a variant pleckstrin homology (PH) domain known as a GLUE domain (44). The structure of the EAP45-GLUE complex with ubiquitin has been determined and shows the typical Ile44-patch mediated interaction (**Figure S3*d***) (2, 12).

SUPPLEMENTARY FIGURE LEGENDS

Figure S1

Ubiquitin recognition in endocytosis and endosomal sorting. (*a*) Domain architecture of Epsin, Eps15, and their yeast orthologs Ent1/2 (represented by Ent1) and Ede1; GGA3; and the Hrs and STAM subunits of ESCRT-0. EH, Eps15 homology. (*b*) Structure of the first UIM of Vps27 (green) in complex with ubiquitin (1Q0W). (*c*) Structure of the Ede1 UBA domain (yellow) in complex with ubiquitin (2G3Q). (*d*) Structure of the VHS domain of STAM1 (green) in complex with ubiquitin (3LDZ). (*e*) Structure of the GAT domain of GGA3 (green) in complex with ubiquitin (1YD8). (*f*) Structure of the Hrs DUIM (green) bound to two ubiquitin molecules in two shades of orange (2D3G). Ubiquitin is orange throughout.

Figure S2

Ubiquitin in RAB5 regulation. (*a*) Domain architecture of Vps9 and Rabex-5. (*b*) Structure of the yeast Vps9 CUE domain dimer bound to ubiquitin (1P3Q). (*c*) Structure of the Rabex-5 A20 zinc finger bound to ubiquitin (2FID). (*d*) Structure of the Rabex-5 MIU bound to -ubiquitinubiquitin (2FID). Compare the N-to-C terminal orientation of the UIM helix to the conventional UIM in **Figure S1*b***.

Figure S3

Ubiquitin recognition in MVB biogenesis. (*a*) Domain architecture of TSG101 (ESCRT-I), yeast Vps36 (ESCRT-II) and human VPS36 (ESCRT-II). (*b*) Structure of the UEV

domain of the ESCRT-I TSG101 subunit in complex with ubiquitin (1S1Q). (*c*) Structure of the TAB2 NZF domain bound to Lys63-diubiquitin (2WWZ), as a model for the yeast ESCRT-II NZF2 complex. (*d*) Structure of the human ESCRT-II GLUE domain bound to ubiquitin (2DX5).

SUPPLEMENTARY REFERENCES

1. Akutsu M, Kawasaki M, Katoh Y, Shiba T, Yamaguchi Y, et al. 2005. Structural basis for recognition of ubiquitinated cargo by Tom1-GAT domain. *FEBS Lett*. 579: 5385-5391
2. Alam SL, Langelier C, Whitby FG, Koirala S, Robinson H, et al. 2006. Structural basis for ubiquitin recognition by the human ESCRT-II EAP45 GLUE domain. *Nat. Struct. Mol. Biol*. 13: 1029-1030
3. Alam SL, Sun J, Payne M, Welch BD, Black BK, et al. 2004. Ubiquitin interactions of NZF zinc fingers. *Embo J* 23: 1411-1421
4. Bilodeau PS, Urbanowski JL, Winistorfer SC, Piper RC. 2002. The Vps27p-Hse1p complex binds ubiquitin and mediates endosomal protein sorting. *Nat. Cell Biol*. 4: 534-539
5. Bilodeau PS, Winistorfer SC, Allaman MM, Surendhran K, Kearney WR, et al. 2004. The GAT domains of clathrin-associated GGA proteins have two ubiquitin-binding motifs. *J. Biol. Chem*. 279: 54808-54816
6. Collins BM, Watson PJ, Owen DJ. 2003. The structure of the GGA1-GAT domain reveals the molecular basis for ARF binding and membrane association of GGAs. *Dev. Cell* 4: 321-332
7. Davies BA, Topp JD, Sfeir AJ, Katzmann DJ, Carney DS, et al. 2003. Vps9p CUE domain ubiquitin binding is required for efficient endocytic protein traffic. *J. Biol. Chem*. 278: 19826-19833
8. Deng Y, Guo Y, Watson H, Au WC, Shakoury-Elizeh M, et al. 2009. Gga2 Mediates Sequential Ubiquitin-independent and Ubiquitin-dependent Steps in the Trafficking of ARN1 from the trans-Golgi Network to the Vacuole. *J. Biol. Chem*. 284: 23830-23841
9. Donaldson KM, Yin HW, Gekakis N, Supek F, Joazeiro CAP. 2003. Ubiquitin signals protein trafficking via interaction with a novel ubiquitin binding domain in the membrane fusion regulator, Vps9p. *Curr. Biol*. 13: 258-262
10. Fisher RD, Wang B, Alam SL, Higginson DS, Robinson H, et al. 2003. Structure and ubiquitin binding of the ubiquitin-interacting motif. *J. Biol. Chem*. 278: 28976-28984
11. Hirano S, Kawasaki M, Ura H, Kato R, Raiborg C, et al. 2006. Double-sided ubiquitin binding of Hrs-UIM in endosomal protein sorting. *Nat. Struct. Mol. Biol*. 13: 272-277
12. Hirano S, Suzuki N, Slagsvold T, Kawasaki M, Trambaiolo D, et al. 2006. Structural basis of ubiquitin recognition by mammalian Eap45 GLUE domain. *Nat. Struct. Mol. Biol*. 13: 1031-1032
13. Hofmann K, Falquet L. 2001. A ubiquitin-interacting motif conserved in components of the proteasomal and lysosomal protein degradation systems. *Trends Biochem. Sci*. 26: 347-350

14. Hong YH, Ahn HC, Lim J, Kim HM, Ji HY, et al. 2009. Identification of a novel ubiquitin binding site of STAM1 VHS domain by NMR spectroscopy. *FEBS Lett*. 583: 287-292
15. Hurley JH, Ren XF. 2009. The circuitry of cargo flux in the ESCRT pathway. *J. Cell Biol*. 185: 185-187
16. Kang RS, Daniels CM, Francis SA, Shih SC, Salerno WJ, et al. 2003. Solution structure of a CUE-ubiquitin complex reveals a conserved mode of ubiquitin binding. *Cell* 113: 621-630
17. Katoh Y, Shiba Y, Mitsuhashi H, Yanagida Y, Takatsu H, Nakayama K. 2004. Tollip and Tom1 form a complex and recruit ubiquitin-conjugated proteins onto early endosomes. *J. Biol. Chem*. 279: 24435-24443
18. Kawasaki M, Shiba T, Shiba Y, Yamaguchi Y, Matsugaki N, et al. 2005. Molecular mechanism of ubiquitin recognition by GGA3 GAT domain. *Genes Cells* 10: 639-654
19. Kostelansky MS, Schluter C, Tam YYC, Lee S, Ghirlando R, et al. 2007. Molecular architecture and functional model of the complete yeast ESCRT-I heterotetramer. *Cell* 129: 485-498
20. Kulathu Y, Akutsu M, Bremm A, Hofmann K, Komander D. 2009. Two-sided ubiquitin binding explains specificity of the TAB2 NZF domain. *Nat. Struct. Mol. Biol*. 16: 1328-1330
21. Lee S, Tsai YC, Mattera R, Smith WJ, Kostelansky MS, et al. 2006. Structural basis for ubiquitin recognition and autoubiquitination by Rabex-5. *Nat. Struct. Mol. Biol*. 13: 264-271
22. Mao YX, Nickitenko A, Duan XQ, Lloyd TE, Wu MN, et al. 2000. Crystal structure of the VHS and FYVE tandem domains of Hrs, a protein involved in membrane trafficking and signal transduction. *Cell* 100: 447-456
23. Mattera R, Puertollano R, Smith WJ, Bonifacino JS. 2004. The trihelical bundle subdomain of the GGA proteins interacts with multiple partners through overlapping but distinct sites. *J. Biol. Chem*. 279: 31409-31418
24. Misra S, Beach BM, Hurley JH. 2000. Structure of the VHS domain of human Tom1 (target of myb 1): Insights into interactions with proteins and membranes. *Biochemistry* 39: 11282-11290
25. Mizuno E, Kawahata K, Kato M, Kitamura N, Komada M. 2003. STAM proteins bind ubiquitinated proteins on the early endosome via the VHS domain and ubiquitin-interacting motif. *Mol. Biol. Cell* 14: 3675-3689
26. Penengo L, Mapelli M, Murachelli AG, Confalonieri S, Magri L, et al. 2006. Crystal structure of the ubiquitin binding domains of rabex-5 reveals two modes of interaction with ubiquitin. *Cell* 124: 1183-1195
27. Pornillos O, Alam SL, Rich RL, Myszka DG, Davis DR, Sundquist WI. 2002. Structure and functional interactions of the Tsg101 UEV domain. *EMBO J*. 21: 2397-2406
28. Prag G, Lee SH, Mattera R, Arighi CN, Beach BM, et al. 2005. Structural mechanism for ubiquitinated-cargo recognition by the Golgi-localized, gamma-ear-containing, ADP-ribosylation-factor-binding proteins. *Proc. Natl. Acad. Sci. U. S. A*. 102: 2334-2339

29. Prag G, Misra S, Jones EA, Ghirlando R, Davies BA, et al. 2003. Mechanism of ubiquitin recognition by the CUE domain of Vps9p. *Cell* 113: 609-620
30. Prag G, Watson H, Kim YC, Beach BM, Ghirlando R, et al. 2007. The Vps27/Hse1 complex is a GAT domain-based scaffold for ubiquitin-dependent sorting. *Dev. Cell* 12: 973-986
31. Puertollano R. 2005. Interactions of Tom1L1 with the multivesicular body sorting machinery. *J. Biol. Chem.* 280: 9258-9264
32. Puertollano R, Bonifacino JS. 2004. Interactions of GGA3 with the ubiquitin sorting machinery. *Nat Cell Biol* 6: 244-251
33. Raiborg C, Bache KG, Gillooly DJ, Madshus IH, Stang E, Stenmark H. 2002. Hrs sorts ubiquitinated proteins into clathrin-coated microdomains of early endosomes. *Nat. Cell Biol.* 4: 394-398
34. Raiborg C, Bremnes B, Mehlum A, Gillooly DJ, D'Arrigo A, et al. 2001. FYVE and coiled-coil domains determine the specific localisation of Hrs to early endosomes. *J. Cell Sci.* 114: 2255-2263
35. Ren X, Kloer DP, Kim YC, Ghirlando R, Saidi LF, et al. 2009. Hybrid structural model of the complete human ESCRT-0 complex. *Structure* 17: 406-416
36. Ren XF, Hurley JH. 2010. VHS domains of ESCRT-0 cooperate in high-avidity binding to polyubiquitinated cargo. *EMBO J.* 29: 1045-1054
37. Sato Y, Yoshikawa A, Yamashita M, Yamagata A, Fukai S. 2009. Structural basis for specific recognition of Lys 63-linked polyubiquitin chains by NZF domains of TAB2 and TAB3. *EMBO J.* 28: 3903-3909
38. Scott PM, Bilodeau PS, Zhdankina O, Winistorfer SC, Hauglund MJ, et al. 2004. GGA proteins bind ubiquitin to facilitate sorting at the trans-Golgi network. *Nat. Cell Biol.* 6: 252-259
39. Shiba T, Kawasaki M, Takatsu H, Nogi T, Matsugaki N, et al. 2003. Molecular mechanism of membrane recruitment of GGA by ARF in lysosomal protein transport. *Nat. Struct. Biol.* 10: 386-393
40. Shiba Y, Katoh Y, Shiba T, Yoshino K, Takatsu H, et al. 2004. GAT (GGA and Tom1) domain responsible for ubiquitin binding and ubiquitination. *J. Biol. Chem.* 279: 7105-7111
41. Shields SB, Oestreich AJ, Winistorfer S, Nguyen D, Payne JA, et al. 2009. ESCRT ubiquitin binding domains function cooperatively during MVB cargo sorting. *J. Cell Biol.* 185: 213-224
42. Shih SC, Katzmann DJ, Schnell JD, Sutanto M, Emr SD, Hicke L. 2002. Epsins and Vps27p/Hrs contain ubiquitin-binding domains that function in receptor endocytosis. *Nat. Cell Biol.* 4: 389-393
43. Shih SC, Prag G, Francis SA, Sutanto MA, Hurley JH, Hicke L. 2003. A ubiquitin-binding motif required for intramolecular monoubiquitylation, the CUE domain. *EMBO J.* 22: 1273-1281
44. Slagsvold T, Aasland R, Hirano S, Bache KG, Raiborg C, et al. 2005. Eap45 in mammalian ESCRT-II binds ubiquitin via a phosphoinositide-interacting GLUE domain. *J Biol Chem* 280: 19600-19606
45. Sundquist WI, Schubert HL, Kelly BN, Hill GC, Holton JM, Hill CP. 2004. Ubiquitin recognition by the human TSG101 protein. *Mol. Cell* 13: 783-789

46. Swanson KA, Hicke L, Radhakrishnan I. 2006. Structural basis for monoubiquitin recognition by the Ede1 UBA domain. *J. Mol. Biol.* 358: 713-724
47. Swanson KA, Kang RS, Stamenova SD, Hicke L, Radhakrishnan I. 2003. Solution structure of Vps27 UIM-ubiquitin complex important for endosomal sorting and receptor downregulation. *EMBO J.* 22: 4597-4606
48. Teo H, Veprintsev DB, Williams RL. 2004. Structural insights into endosomal sorting complex required for transport (ESCRT-I) recognition of ubiquitinated proteins. *J. Biol. Chem.* 279: 28689-28696
49. Wang QH, Young P, Walters KJ. 2005. Structure of S5a bound to monoubiquitin provides a model for polyubiquitin recognition. *J. Mol. Biol.* 348: 727-739
50. Wollert T, Hurley JH. 2010. Molecular mechanism of multivesicular body biogenesis by ESCRT complexes. *Nature* 464: 864-873
51. Zhu GY, Zhai P, He XY, Terzyan S, Zhang RG, et al. 2003. Crystal structure of the human GGA1 GAT domain. *Biochemistry* 42: 6392-6399

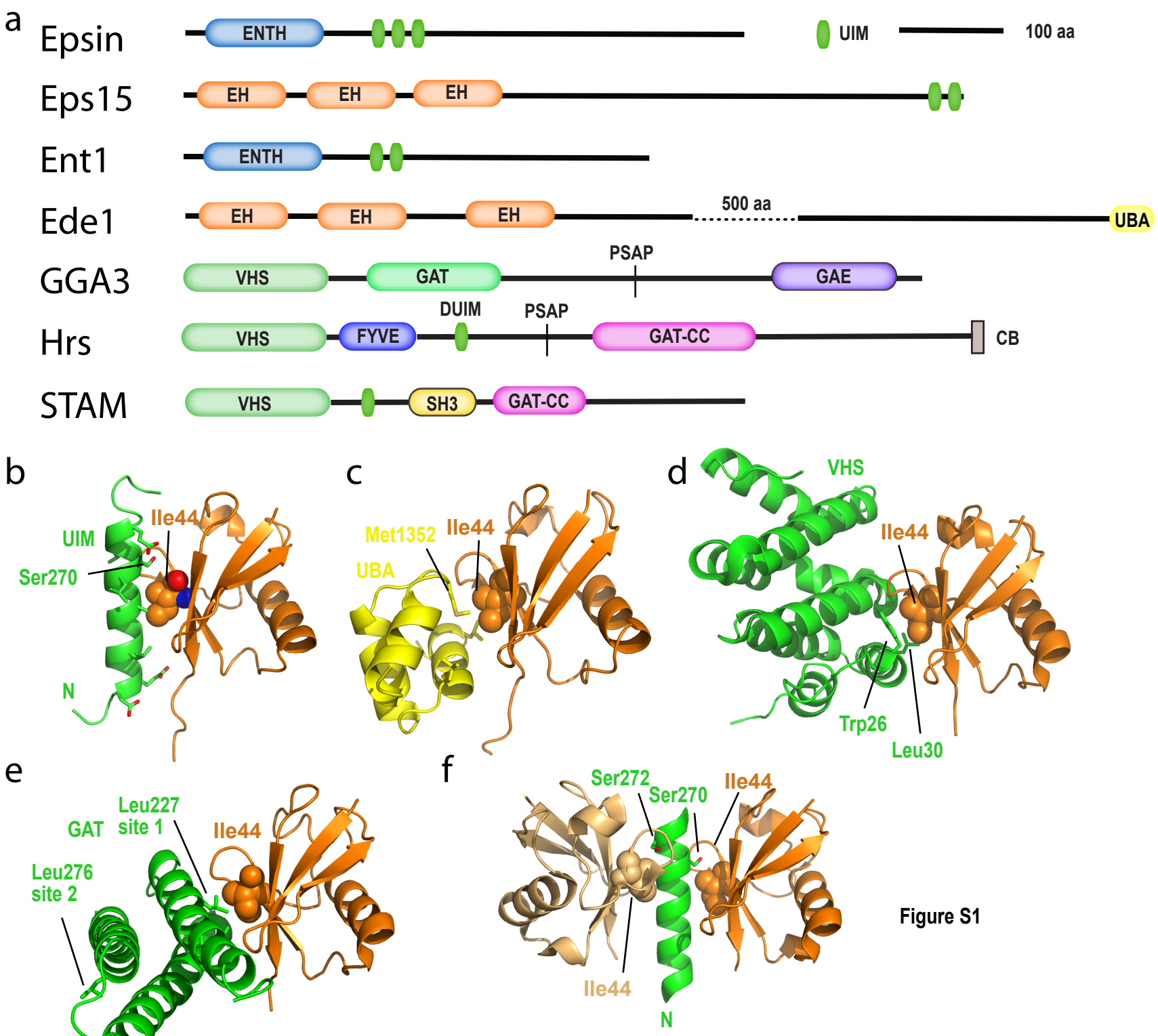
a
Epsin
ENTH
UIM
100 aa
Eps15
EH
EH
EH
Ent1
ENTH
Ede1
EH
EH
EH
500 aa
UBA
GGA3
VHS
GAT
PSAP
GAE
Hrs
VHS
FYVE
DUIM
PSAP
GAT-CC
CB
STAM
VHS
SH3
GAT-CC
b
UIM
Ile44
Ser270
N
c
Met1352
Ile44
UBA
d
VHS
Ile44
Trp26
Leu30
e
GAT
Leu227
site 1
Ile44
Leu276
site 2
f
Ser272
Ser270
Ile44
Ile44
N

Figure S1

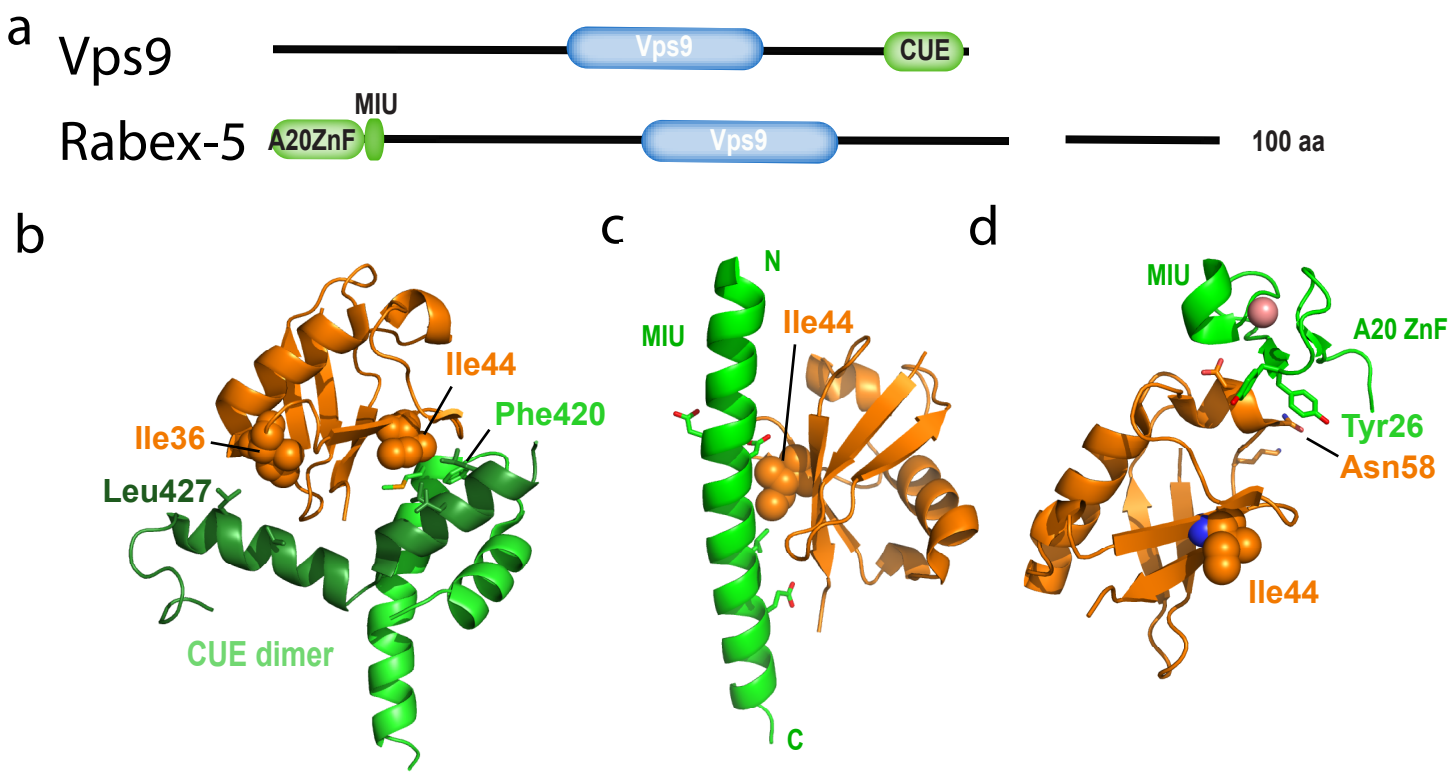
a
Vps9
Vps9
CUE
MIU
Rabex-5
A20ZnF
Vps9
100 aa
b
Ile44
Phe420
Ile36
Leu427
CUE dimer
c
N
MIU
Ile44
C
d
MIU
A20 ZnF
Tyr26
Asn58
Ile44

Figure S2

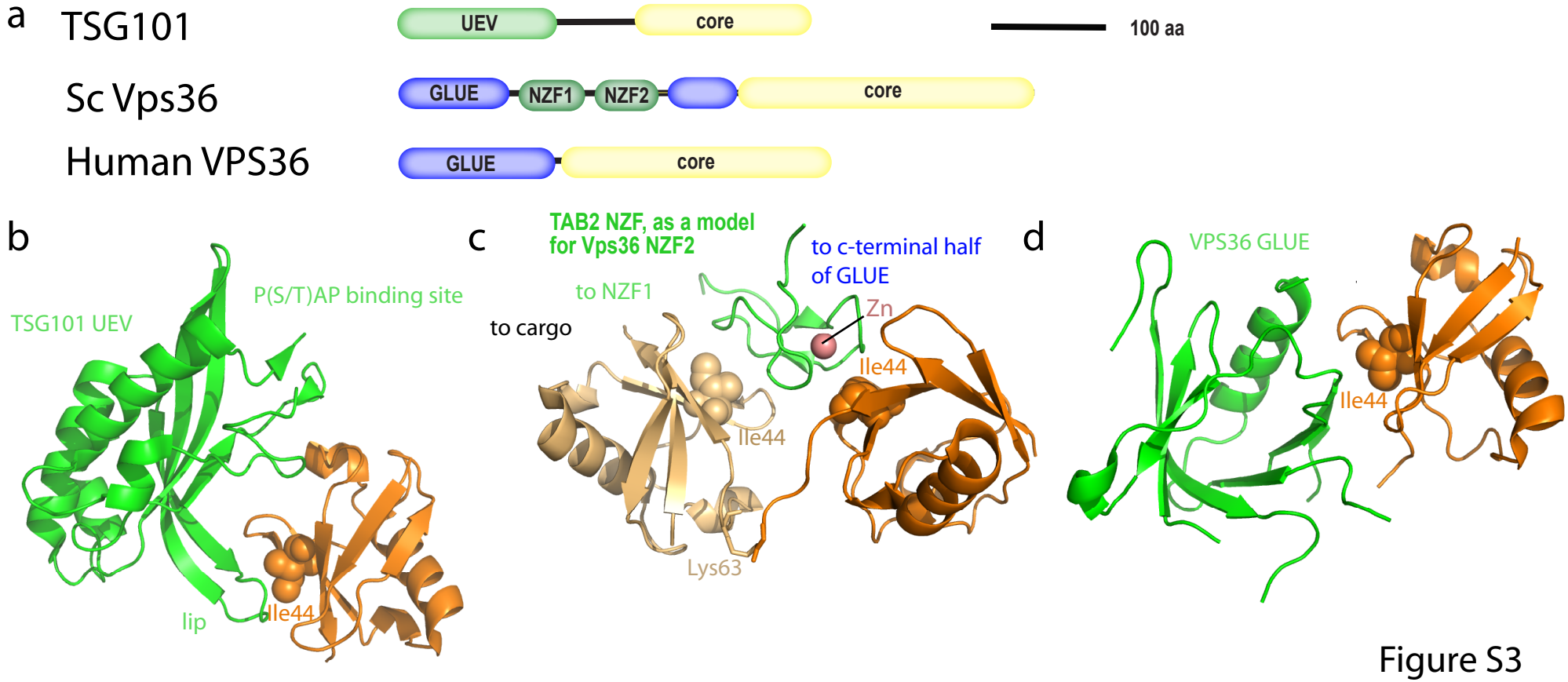
a
TSG101
UEV
core
100 aa
Sc Vps36
GLUE
NZF1
NZF2
core
Human VPS36
GLUE
core
b
TSG101 UEV
P(S/T)AP binding site
lip
Ile44
c
TAB2 NZF, as a model
for Vps36 NZF2
to c-terminal half
of GLUE
to NZF1
to cargo
Zn
Ile44
Ile44
Lys63
d
VPS36 GLUE
Ile44

Figure S3